Subnuclear distribution of the largest subunit of the human origin recognition complex during the cell cycle

Maria Rosa Lidonnici[1], Rossella Rossi[1], Sonia Paixão[1], Ramiro Mendoza-Maldonado[2], Roberta Paolinelli[3], Caterina Arcangeli[3], Mauro Giacca[2,3], Giuseppe Biamonti[1] and Alessandra Montecucco[1,*]

[1]Istituto di Genetica Molecolare, CNR, Via Abbiategrasso 207, 27100 Pavia, Italy
[2]Molecular Medicine Laboratory, International Centre for Genetic Engineering and Biotechnology, Padriciano 99, 34012 Trieste, Italy
[3]NEST/INFM and Scuola Normale Superiore, Piazza dei Cavalieri 7, 56126 Pisa, Italy
*Author for correspondence (e-mail: montecucco@igm.cnr.it)

Summary

In eukaryotes, initiation of DNA replication requires the activity of the origin recognition complex (ORC). The largest subunit of this complex, Orc1p, has a critical role in this activity. Here we have studied the subnuclear distribution of the overexpressed human Orc1p during the cell cycle. Orc1p is progressively degraded during S-phase according to a spatio-temporal program and it never colocalizes with replication factories. Orc1p is resynthesized in G1. In early G1, the protein is distributed throughout the cell nucleus, but successively it preferentially associates with heterochromatin. This association requires a functional ATP binding site and a protein region partially overlapping the bromo-adjacent homology domain at the N-terminus of Orc1p. The same N-terminal region mediates the in vitro interaction with heterochromatin protein 1 (HP1). Fluorescence resonance energy transfer (FRET) experiments demonstrate the interaction of human Orc1p and HP1 in vivo. Our data suggest a role of HP1 in the recruitment but not in the stable association of Orc1p with heterochromatin. Indeed, the subnuclear distribution of Orc1p is not affected by treatments that trigger the dispersal of HP1.

Supplementary material available online at
http://jcs.biologists.org/cgi/content/full/117/22/5221/DC1

Key words: ORC, Eukaryotic DNA replication, Heterochromatin, HP1, FRET

Introduction

The origin recognition complex (ORC) is a complex of six different subunits, named Orc1p to 6p, that was initially isolated for its ability to bind to the autonomously replicating sequences (ARS) of *Saccharomyces cerevisiae* in an ATP-dependent manner (Bell and Stillman, 1992). Subsequently similar complexes have been identified in all eukaryotic species, including humans. There is much evidence to support the role of ORC in initiation of DNA replication. Indeed, individual Orc subunits are required for DNA replication in budding yeast, for cell proliferation and chorion gene amplification in *Drosophila melanogaster* and for in vitro DNA replication in *Xenopus laevis* egg extracts (reviewed by Bell and Dutta, 2002; Biamonti et al., 2003). According to the current model, ORC acts as a 'landing pad' for the stepwise assembly of the pre-replication complex (pre-RC) on the origins of DNA replication. In budding yeast, ORC is bound to the origin sequence throughout the cell cycle but in mammalian cells the association of ORC proteins to DNA is less well defined. However, it has been recently shown that Orc1p and Orc2p interact with true DNA replication origins in human cells (Abdurashidova et al., 2003; Ladenburger et al., 2002; Paixão et al., 2004).

Some laboratories have reported that the level of human Orc1p oscillates during the cell cycle and the protein is degraded in S-phase (Kreitz et al., 2001; Mendez et al., 2002; Tatsumi et al., 2003). In contrast, other groups have found that the Orc1p level is constant in the cell cycle in human and hamster cell lines (Li and DePamphilis, 2002; Okuno et al., 2001; Thome et al., 2000). Evidence accumulated in the past few years indicates that the function of ORC extends beyond DNA replication. The clearest example of an alternate function is the role of ORC in the transcriptional repression of the silent mating type loci, HMR and HML, in *S. cerevisiae*. Paradoxically, in this case ORC participates in the assembly of the chromatin conformation that eventually suppresses the activity of the origin (Vujcic et al., 1999). The ability of ORC to promote the formation of transcriptionally silent, late-replicating, chromosomal domains has also been recently demonstrated for the yeast rDNA locus by means of the dynamic molecular combing technique (Pasero et al., 2002). In both cases, transcriptional silencing and origin inactivation depend on the interaction of ORC with Sir proteins. The ability of ORC to interact with heterochromatin markers and to direct their recruitment to silent portions of the genome seems to be evolutionary conserved. However, there is no evidence so far that this is true in mammalian cells. In *Xenopus* and *Drosophila*, Orc1p binds heterochromatin protein 1 (HP1), which is functionally analogous to Sir1p of budding yeast. In vitro studies have shown that both the yeast and the *Drosophila*

Orc1p interact with Sir1/HP1 through their N-terminal portion (Pak et al., 1997; Zhang et al., 2002a). This region overlaps a bromo-adjacent homology (BAH) domain that Orc1 proteins share with Sir3p and other chromatin-associated proteins such as DNA methyl-transferases. Collectively these findings support the hypothesis that ORC could also be involved in the establishment and maintenance of chromatin domains.

Here we analyzed the subnuclear distribution of the overexpressed human Orc1p (Orc1p*) during the cell cycle. Although the protein is distributed throughout the cell nucleus in early G1, in mid and late G1 it preferentially associates with heterochromatin. The level of Orc1p* decreases during S-phase and the protein never colocalizes with replication factories suggesting a link between protein degradation and displacement from replicating chromatin. The association with heterochromatin requires a functional ATP binding site and the protein region that mediates the in vitro interaction with HP1. As FRET analysis detects an interaction between the two proteins in vivo we suggest a role of HP1 in the recruitment of Orc1p to heterochromatin.

Materials and Methods

Drugs, cell culture and cell treatment

HeLa, COS7 and NIH-3T3 cells were grown as monolayers in complete Dulbecco's modified Eagle's medium (DMEM) supplemented with 10% fetal calf serum, 4 mM glutamine and 50 μg/ml gentamicin. Exponentially growing cells were transfected using FUGENE 6 transfection reagent (Roche, Germany). Routinely we used 1 μg of plasmid DNA for 3×10^5 cells. 24 or 48 hours after transfection cells were analyzed by western blotting and/or immunofluorescence. Synchronization of HeLa cells in mitosis was obtained by growing cells in 40 ng/ml nocodazole (Sigma, St Louis, CA) for 16 hours as previously described (Rossi et al., 1999). For NIH-3T3 synchronization, cells were grown for 20 hours in 100 ng/ml nocodazole. For synchronization in G1 phase, mitotic cells were shaken off and released in fresh medium for different times. HeLa and NIH-3T3 cells were incubated for 6 hours in trichostatin A (TSA; Sigma) containing medium at the concentrations indicated in the text. RNase treatment was as previously described (Chiodi et al., 2000). Briefly, cells grown on coverslips were incubated at 4°C for 10 minutes in extraction buffer (100 mM NaCl, 300 mM sucrose, 10 mM PIPES pH 6.8, 3 mM $MgCl_2$, 2 mM vanadylribonucleaside complexes, 0.5% Triton X-100 and the following protease inhibitors: 2 μg/ml aprotinin, 1 μg/ml leupeptin, 1 μg/ml pepstatin A, 0.2 mM AEBSF) and for an additional 10 minutes in the same buffer with 250 mM ammonium sulfate. After washing, cells were incubated for 20 minutes at 37°C with 25 μg/ml RNase A (Roche) and then subjected to immunofluorescence.

Plasmids

The human Orc1 and Orc2 cDNAs were obtained by RT-PCR amplification from total RNA of human HeLa cells and cloned as BamHI-XbaI and KpnI-XhoI fragments into the pcDNA3 vector (Invitrogen, USA) respectively. The human HP1α cDNA was obtained from a Superscript normal human prostate cDNA library on the pCMV•SPORT6 vector (Life Technology). To express the Orc1-GFP fusion, human Orc1 cDNA was cloned in-frame at the N-terminus of the GFP ORF in pEGFP-N1 vector (Clontech, USA). To obtain the Orc1-Flag fusion the human Orc1 cDNA was cloned into SacI-SalI sites of pIRES-hrGFP-2a plasmid (Stratagene, Carlsbad, CA). This vector contains a dicistronic expression cassette in which the multicloning site is followed by the internal ribosomal entry site (IRES) of the encephalomyocarditis (EMCV) virus linked to the humanized recombinant GFP coding sequence. This allows the expression of the gene of interest fused to the Flag epitope to be monitored at the single-cell level owing to the translation of the GFP from the same transcript. GFP and Flag-tagged mutants of Orc1 were generated by two-step PCR-mediated mutagenesis with suitable primers, as previously described (Montecucco et al., 1998). Restriction enzymes were purchased from Promega, Madison, WI. Oligonucleotides were purchased from MWG-Biotech AG (Germany). Plasmids were verified by DNA sequencing (Thermo Sequenase™Cy$^{5.5}$ Amersham Bioscience). pGEX2T-HP1α was obtained from pCMV•SPORT6-HP1α by PCR amplification and cloning of a BamHI-EcoRI fragment into pGEX-2T (Amersham Bioscience). The Orc1 deletion mutants for the GST pull-down assays (1-144, 151-269, 270-861) were obtained as HindIII-KpnI fragments from the respective GFP fusions and cloned into the pcDNA3 vector for in vitro transcription. The Orc1 C-terminal mutant 529-861 was obtained as an EcoRI-XbaI fragment from plasmid pcDNA3-Orc1 and subcloned into the same vector. pEGFP-HP1α was obtained by PCR amplification of pCMV•SPORT6-HP1α and cloning of an EcoRI-BamHI fragment into pEGFP-C1 (Clontech) digested with EcoRI-BglII. pBFP-Orc1 was obtained by recovering the Orc1 segment from pEGFP-Orc1 as an HindIII-MluI fragment followed by cloning into the pBFP-C1 vector (Clontech). pEGFP-Orc2 was obtained by PCR amplification of pCDNA3-Orc2 and cloning of a KpnI-SmaI fragment into pEGFP-C1.

Cell cycle profile analysis of Orc1-GFP-transfected cells

HeLa cells were transiently transfected with pOrc1-EGFP plasmid by the calcium phosphate method in six-well culture plates (Corning). 48 hours after transfection, cells were collected and analyzed by double-cytofluorometric analysis on a FACSCalibur (Becton Dickinson). Cells were analyzed for cell cycle profile (DNA content) by incorporation of propidium iodide solution (Sigma), and simultaneously for Orc1-GFP expression.

Immunofluorescence

Cells grown on coverslips were rinsed with cold PBS, fixed for 10 minutes in 2% paraformaldehyde and permeabilized in PBS-0.5% Triton X-100 for 10 minutes at 4°C. When required, soluble proteins were extracted by incubating the cells for 2 minutes on ice in CSK buffer (10 mM HEPES-KOH, pH 7.4, 100 mM NaCl, 300 mM sucrose, 3 mM $MgCl_2$, 0.5% Triton X-100 and protease inhibitors). Epitope-tagged proteins were detected with the anti-Flag polyclonal antibody (Santa Cruz Biotechnologies, Santa Cruz, CA). HP1-proteins (α, β) were revealed with the anti-mouse M31/human HP1β antibody (Serotec, UK) and mouse anti-HP1α monoclonal antibody (Chemicon International, Temecula, CA). For PCNA detection with PC10 monoclonal antibody (Santa Cruz Biotechnologies) cells were fixed with paraformaldehyde and permeabilized with cold methanol as previously described (Montecucco et al., 1998). Primary antibodies were diluted at working concentration in PBS containing 2% skimmed milk (DIFCO, USA). After 1 hour at 37°C in a humid chamber, coverslips were washed three times with PBS. Secondary antibodies used were: TRITC-conjugated anti-rabbit IgG, Cy5-conjugated anti-rabbit IgG, Cy5-conjugated anti-rat IgG, FITC-conjugated anti-rat IgG, TRITC-conjugated anti-mouse IgG (all from Jackson ImmunoResearch Lab, UK). DNA was stained with 0.1 μg/ml 4,6′-diamino-2-phenylindole (DAPI; Sigma). Conventional epifluorescence microscopy was performed with a Leitz Orthoplan microscope equipped with a 50× objective. Photomicrographs were taken with Camedia digital camera C-3030 (Olympus). Confocal microscopy was performed with a Leica TCS SP2 confocal laser microscopy apparatus equipped with a 63×/NA=1.32 oil immersion objective. We used the 488-nm laser line for excitation of FITC and GFP (detected at 500 nm<λ_{FITC}<540 nm), the 543-nm laser line for

TRITC fluorescence (detected at λ>570 nm) and the 633-nm laser line for excitation of Cy5 (detected at 650<λ_{Cy5}<700 nm). Images were exported to Adobe Photoshop (Adobe, San Jose, CA).

Cell extracts, chromatin isolation, western blotting and co-immunoprecipitation

To prepare total cell extracts, cells were harvested by centrifugation (5 minutes, 1300 *g*, 4°C) resuspended in Laemmli buffer, and boiled for 10 minutes as previously described (Montecucco et al., 2001). Nuclear extracts and chromatin were prepared as described (Mendez and Stillman, 2000). Briefly, cells were resuspended at a concentration of 15×10⁶ cells/ml in hypotonic buffer (20 mM HEPES-KOH, pH 8.0, 5 mM MgCl₂, 0.1 mM dithiothreitol and protease inhibitors). After 30 minutes on ice, nuclei were collected by centrifugation and resuspended in the nuclear extraction buffer (15 mM Tris-HCl, pH 7.5, 1 mM EDTA, 0.4 M NaCl, 10% sucrose, 1 mM DTT and protease inhibitors). After 30 minutes at 4°C, insoluble proteins were removed by centrifugation. To isolate the chromatin fraction, HeLa cells were resuspended (4×10⁷ cells/ml) in buffer A (10 mM HEPES, pH 7.9, 10 mM KCl, 1.5 MgCl₂, 0.34 M sucrose, 10% glycerol, 1 mM dithiothreitol and protease inhibitors) plus 0.1% Triton X-100. Cells were incubated for 5 minutes on ice. Nuclei were collected in pellet 1 (P1) by low-speed centrifugation. Nuclei were washed and lyzed in hypotonic buffer B (3 mM EDTA, 0.2 mM EGTA, 1 mM dithiothreitol and protease inhibitors) that induces nuclear swelling. Insoluble chromatin (P3) was collected by centrifugation.

Western blot analysis was performed as previously described (Montecucco et al., 2001). The following primary antibodies were used for detection of protein antigens: Flag-probe (D8) polyclonal antibody (Santa Cruz Biotechnologies); anti-Orc1 and anti-Orc2 polyclonal antibodies kindly supplied by Bruce Stillman (CSH Lab, USA); anti-cyclin E monoclonal antibody (Santa Cruz Biotechnologies); anti-cyclin A monoclonal antibody (Sigma); anti-α-tubulin monoclonal antibody (Sigma). Primary antibodies were revealed with horseradish peroxidase-conjugated goat anti-mouse or anti-rabbit antibodies and enhanced chemiluminescence systems (Super Signal West Dura Extended, Pierce, Rockford, IL and ECL, Amersham Bioscience).

For co-immunoprecipitation experiments, nuclear extract was prepared from G1-phase HeLa cells expressing Orc1-Flag. The extract was incubated with anti-Flag M2 affinity gel (Sigma) for 1 hour at 4°C. The immunoprecipitated material was analyzed by western blotting with the anti-Flag and anti-Orc2 polyclonal antibodies.

Recombinant GST fusion proteins and in vitro binding assays

[³⁵S]-labeled proteins were produced in vitro by using a coupled transcription-translation system (TNT/T7/Sp6 coupled reticulocyte lysed system, Promega) according to the manufacturer's instructions. Pull-down experiments using the recombinant GST-HP1α and GST proteins were performed as described (Marcello et al., 2003; Marzio et al., 1998).

Fluorescence resonance energy transfer (FRET)

Cells were transiently transfected with expression plasmids for HP1α, Orc1p and Orc2p fused to different fluorescent proteins by the calcium phosphate method in LabTek II four-chamber glass slides (Nalgene). Cells were fixed in 2% paraformaldehyde after 48 hours and mounted directly in 70% glycerol for FRET analysis. FRET measurements were carried out with an epifluorescence Axioskop 2 Zeiss microscope mounting a 103 W HBO lamp, a 100×/NA=1.3, oil-immersion Plan-Neofluar objective and Nomarsky optics, performed as described in detail elsewhere (Marcello et al., 2001; Marcello et al., 2003). Briefly, FRET experiments consisted of collecting two EGFP emission signals by exciting the EGFP with two different excitation wavelengths, 480 and 350 nm, the former being optimal for EGFP and the latter for BFP. The background fluorescence was measured for each field outside of the transfected cells and subtracted. The existence of FRET was inferred by determining the ratio between EGFP fluorescence following excitation at 350 nm to that following excitation at 480 nm. When evaluating these FRET ratios, emission intensities were scaled to take into account the different detection time. Data acquisition and analysis were performed using the MetaMorph software (Universal Imaging Corporation).

Chromatin Immunoprecipitation (ChIP)

3×10⁷ exponentially growing HeLa cells were transfected with Orc1-Flag and synchronized in G1 as described above. Cells were crosslinked for 3 minutes with 1% formaldehyde (Merck). Chromatin was purified and then fractionated through a Cesium chloride density gradient as previously described (Frouin et al., 2002; Paixão et al., 2004). After dialysis against 50 mM Tris-HCl pH 8, 150 mM NaCl and 5 mM EDTA, chromatin was immunopurified with 10 μg anti-Flag M2 affinity gel (Sigma) or 10 μg anti-immunoglobulin G (IgG) (SantaCruz biotechnology) antibody as negative control. The immunopurified chromatin was incubated in PK buffer (0.5% SDS, 100 mM NaCl, 300 μg/ml proteinase K) for 3 hours at 56°C. Crosslinking was reverted at 65°C for 6 hours. DNA was purified by standard phenol-chloroform extraction and ethanol precipitation and dissolved in 50 μl of TE buffer. DNA was then analyzed by competitive PCR.

Competitive PCR analysis

Competitive PCR was performed using primer sets B48 (B48II Dx, 5′-GACTGGAAACTTTTTTGTAC-3′; B48 Sx, 5′-TAGCTACAC-TAGCCAGTGACCTTTTTCC-3′) and B13 (B13 Dx, 5′-GCCA-GCTGGGTGGTGATAGA-3′; B13 Sx, 5′-CCTCAGAACCCAG-CTGTGGA-3′). A constant volume of immunopurified DNA was co-amplified with decreasing amounts of competitor template for 40 cycles. The competitor consists of a 130 bp stuffer DNA flanked by the target sequences for B13 and B48 primer sets and was obtained as previously described (Giacca et al., 1994). Amplification products were resolved on 10% PAGE and stained with ethidium bromide. The intensity of the amplification band was quantified with the NIH-Image program (version 1.62).

Results

The subnuclear distribution of Orc1p changes during the cell cycle

The subnuclear distribution of Orc1p has been poorly investigated. We decided to study this aspect using the overexpressed human protein (Orc1p*). As a starting point we verified the ability of Orc1p* to behave as the endogenous protein. In particular, Orc1p* (fused to the Flag epitope) associated with chromatin, interacted with the endogenous Orc2p subunit of ORC and its level oscillated during the cell cycle being minimal in S and G2/M phases (see Fig. S1 in supplementary material). More importantly, Orc1p* was able to bind in vivo to the lamin B2 origin of DNA replication, one of the few human DNA sequences shown to interact with ORC in vivo (Abdurashidova et al., 2003; Ladenburger et al., 2002; Paixão et al., 2004). This was assessed by chromatin immunoprecipitation (ChIP) analysis of HeLa cells transiently transfected with Orc1-Flag. After in vivo crosslinking, chromatin was immunoprecipitated with the anti-Flag antibody and the immunopurified DNA was used in competitive PCR to determine the abundance of the lamin B2 origin (B48 in Fig.

Fig. 1. Chromatin immunoprecipitation (ChIP) analysis of HeLa cells transiently transfected with Orc1-Flag. (A) Schematic representation of the genomic region comprising the origin of DNA replication associated to the lamin B2 and TIMM 13 genes. The origin sequence is recognized by B48 primers. The control B13 region is also indicated. (B) Crosslinked chromatin was immunopurified with anti-Flag (α-Flag) or with a control non-specific antibody (α-IgG). After reversion of crosslinking, immunopurified DNA was subjected to competitive PCR with B48 and B13 primer sets. Dilutions of the competitor DNA (see Materials and Methods) are indicated above each lane. The identity of the amplification bands is indicated on the right of each panel. The relative abundance of B48 and B13 sequences in the immunopurified DNA is determined by the ratio of genomic (G) to competitor (C) bands. (C) Histogram showing the enrichment of B48 over B13 sequences in the immunopurified DNA obtained with α-Flag and α-IgG antibodies. Bar indicates the variation seen in three independent experiments.
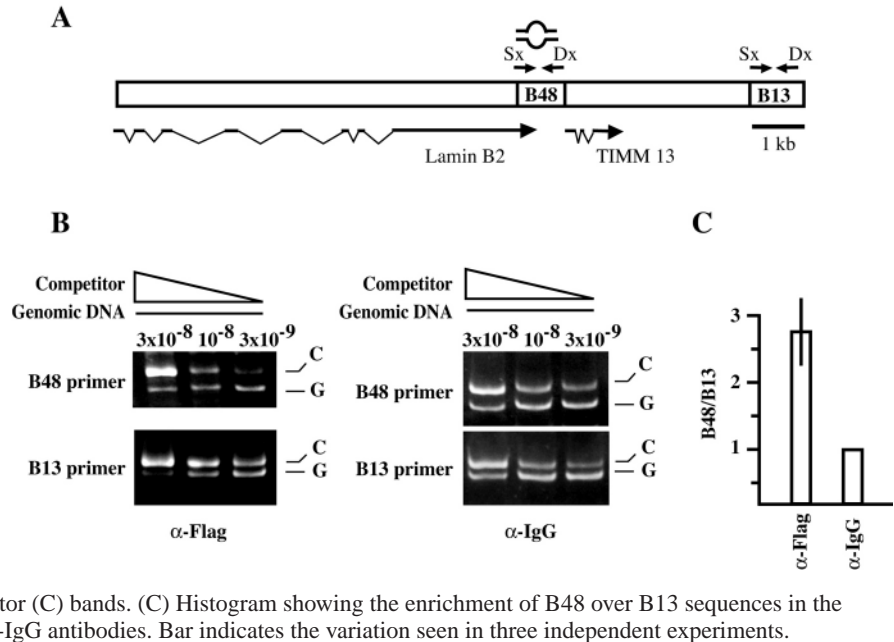
1) relative to that of a non-origin sequence which is not bound by ORC (B13 in Fig. 1). Competitive PCR is based on the co-amplification of a fixed amount of immunopurified genomic DNA, with unknown concentration, and decreasing amounts of a competitor template. The genomic and the competitor sequences are recognized by the same primer set. Because the competitor is 35 bp longer than the genomic sequence, co-amplification results in the production of two DNA fragments that can be resolved by gel electrophoresis (Fig. 1B). The 1:1 ratio between the competitor and genomic bands provides a measure of the amount of the genomic sequence in the immunopurified material. As shown in Fig. 1B, the 1:1 ratio was obtained at a 10^{-8} dilution of the competitor for B48 sequence and at 3×10^{-9} for B13, indicating a threefold enrichment of the origin over the B13 sequence in the immunopurified DNA (Fig. 1C). As this value is comparable to that measured for the same region after immunoprecipitation of the endogenous Orc proteins (Ladenburger et al., 2002; Paixão et al., 2004) the results in Fig. 1C support the conclusion that Orc1p* associates with pre-replication complexes assembled on chromosomal DNA replication origins.

Based on these results we investigated the distribution of Orc1p*, tagged either at the amino- or at the carboxyl-terminus with Flag or GFP, in human HeLa, monkey COS7 and mouse NIH-3T3 cells. In all cell lines, the protein showed diffuse nuclear staining with a few sites of preferential accumulation that overlapped pericentric heterochromatin intensely decorated with DAPI (Fig. 2A). This pattern was observed 24 hours and 48 hours after transfection (not shown). The association with heterochromatin was confirmed by the colocalization with heterochromatin protein 1 (HP1) (Jones et al., 2000; Maison et al., 2002) (Fig. 2B). Thus, the association with heterochromatin of Orc1p* occurs in cell lines of different mammalian species and is not influenced by the position and type of the tag (Flag compared to GFP).

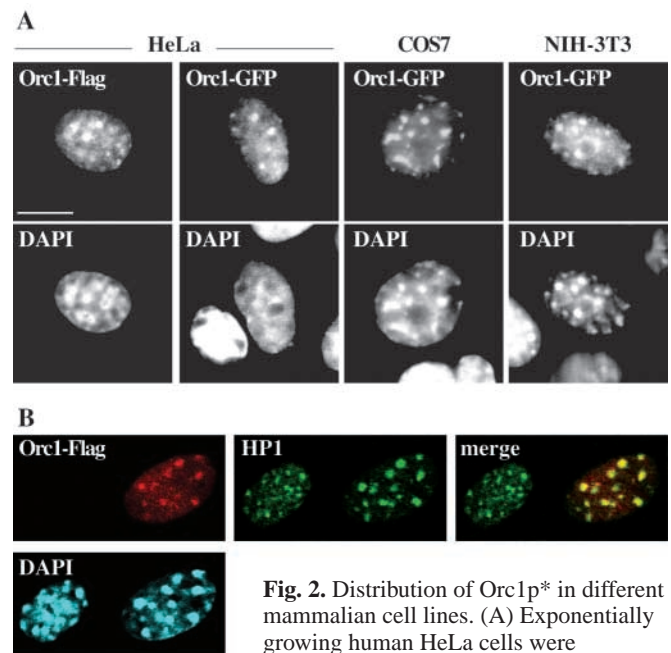We next investigated the distribution of Orc1p* during the

Fig. 2. Distribution of Orc1p* in different mammalian cell lines. (A) Exponentially growing human HeLa cells were transfected with either Orc1-Flag or Orc1-GFP. After 48 hours, cells were fixed and processed for conventional microscopy. The distribution of Orc1-Flag was revealed with the rabbit anti-Flag antibody and a TRITC-conjugated anti-rabbit secondary antibody. The localization of Orc1-GFP was revealed by GFP fluorescence. Cells were counterstained with DAPI. The distribution of Orc1-GFP was also determined in transfected monkey COS7 and mouse NIH-3T3 cells. (B) Asynchronous NIH-3T3 cells were transfected with Orc1-Flag and after 48 hours were fixed and stained with the rabbit anti-Flag and the rat anti-HP1β antibodies. Antigen-antibody complexes were revealed with a TRITC-conjugated anti-rabbit secondary antibody and with a Cy5-conjugated anti-rat secondary antibody (visualized in green). Nuclei were stained with DAPI. Confocal images of the same field were taken. Bar, 10 μm.
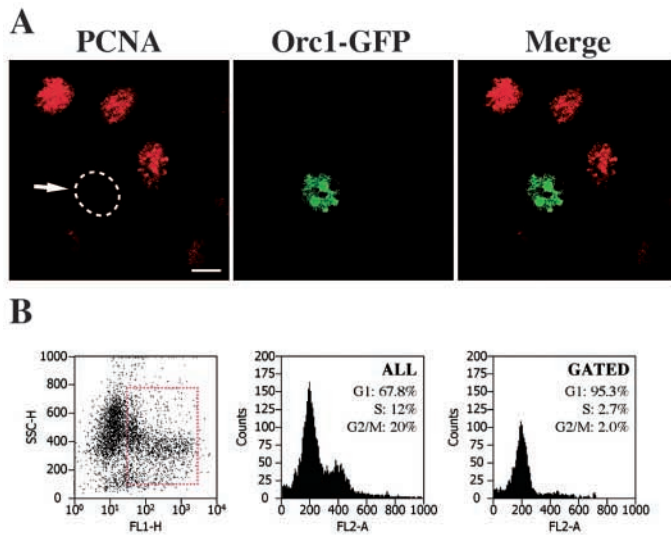
Fig. 3. Orc1p* labels G1 cells. (A) HeLa cells expressing Orc1-GFP were stained with the anti-PCNA PC10 monoclonal antibody and with the anti-mouse Cy5-conjugated secondary antibody (red). The fluorescent signal of the Orc1-GFP fusion (green) is also shown. Confocal laser images of the same field were taken and merged. The arrow indicates a PCNA-negative nucleus expressing Orc1-GFP. Bar, 10 μm. (B) FACS analysis. The FACS profile in the left side panel shows the fluorescence of the total cell population 48 hours after transfection. The gate (dotted line) shows the sub-population of transfected cells expressing Orc1-GFP (29% of total). The other two panels show the DNA content of the total cell population (ALL) and of cells expressing Orc1-GFP (GATED). The distribution of the cells in the cell cycle according to the DNA content is indicated on the right side of each panel.

cell cycle. HeLa cells expressing Orc1-GFP were stained with antibodies against the replicative factor PCNA (proliferating cell nuclear antigen) that associates with replication factories in S phase but is almost undetectable in G1 nuclei. Most Orc1-GFP positive cells were in G1 phase as indicated by the lack of PCNA staining (Fig. 3A) and by FACS analysis (Fig. 3B). This result is consistent with the degradation of the protein during S phase (see Fig. S1C in supplementary material) (Mendez et al., 2002; Tatsumi et al., 2003). To investigate this aspect in more detail, we cloned Orc1-Flag into pIRES-hrGFP-2a, a vector that directs the production of a dicistronic transcript in which the gene of interest and the GFP sequence are separated by an internal ribosomal entry site (IRES) (Fig. 4A). Exponentially growing HeLa cells were transiently

Table 1. Cell-cycle regulation of overexpressed Orc1p

	GFP (+)*	
	Flag (+)[†] 65±4%	Flag (–)[‡] 35±4%
PCNA (+)	14±3%	100%
PCNA (–)	86±3%	–

*HeLa cells transfected with the pIRES-hrGFP plasmid expressing GFP.
[†]Transfected cells in which Orc1-Flag was detectable.
[‡]Transfected cells in which Orc1-Flag was undetectable. Two hundred GFP-expressing cells per experiment were scored in three independent experiments.

transfected with pOrc1-Flag/GFP and analyzed by confocal laser microscopy to reveal the distribution of Orc1-Flag, the reporter GFP protein and the endogenous PCNA. In this assay GFP visualized transfected cells, and in fact cells expressing Orc1-Flag were always GFP-positive. In contrast, as reported in Table 1 and shown in Fig. 4B, a fraction of GFP-positive cells was not stained by the anti-Flag antibody. As indicated by the PCNA subnuclear distribution these cells were in mid/late S and G2 phases. A similar pattern was observed in mouse NIH-3T3 cells (see Fig. S2 in supplementary material). About 14% of Flag-positive cells displayed PCNA in the typical early S-phase pattern (Table 1 and Fig. 4C). In these cells Orc1p* and PCNA occupied mutually exclusive nuclear areas (Fig. 4C). Collectively these results are consistent with a model whereby origin firing is accompanied by the displacement of Orc1p from chromatin and its successive degradation.

As Orc1p* displays a similar distribution in human and mouse cells (Fig. 2A, Fig. 4B; see also Fig. S2 in supplementary material) we decided to investigate its subnuclear localization during G1 phase in NIH-3T3 cells that are more suitable for visualization of heterochromatic foci. Transfected cells were synchronized in mitosis with nocodazole and then released for increasing time intervals in G1. As expected from the degradation of Orc1p* during S phase (Fig. 4; see also Figs S1 and S2 in supplementary material), most of the cells transfected with pOrc1-Flag/GFP (more than 95%) were not stained by anti-Flag antibodies when blocked at the mitotic spindle checkpoint with nocodazole (see Fig. S3 in supplementary material). As shown in Fig. 5, in early G1 (2 hours after the release from nocodazole block) Orc1-Flag was not associated with heterochromatic foci stained by DAPI and by the anti-HP1 antibody. Instead, colocalization with heterochromatin was detectable in 35% of mid G1 (Fig. 5, 6 hours) and in 65% of late G1 (9 hours, not shown) cells.

Protein determinants involved in Orc1p* focalization

Based on the results in the previous section we sought to identify the determinants responsible for the association of Orc1p* with heterochromatin. In all species, Orc1p has a modular structure with a BAH and an ATPase domain located at the N- and C-terminal regions of the protein, respectively. We expressed different portions of Orc1p, tagged with either GFP or Flag, in NIH-3T3 cells. This analysis showed that the region from position 151 to 269, partially overlapping the BAH domain, was necessary for Orc1p focalization (see Δ151-269 in Fig. 6A,B). The same result was obtained in human HeLa cells (see Fig. S4 in supplementary material). However, a mutant lacking the first 150 amino acids [(151-861)-GFP] was still recruited to heterochromatin ruling out the involvement of the BAH domain (Fig. 6A). We produced further internal deletion mutants to map more precisely the determinant directing the association with heterochromatin. Surprisingly, two reciprocal mutants (Δ151-231 and Δ232-269) both colocalized with DAPI foci suggesting the existence of functionally redundant sequences involved in Orc1p* focalization. Although necessary, the 151-269 region was unable to direct the reporter GFP to heterochromatin [see (151-269)-GFP and (1-269)-GFP in Fig. 6A], indicating the involvement of additional motifs. As stated above, the C-terminal part Orc1p contains an ATPase domain

comprising Walker A and Walker B motifs. In *S. cerevisiae,* substitution of lysine 485 in the Walker A motif with threonine abrogates ATP binding, whereas replacement of aspartic acid 569 in the Walker B motif with tyrosine reduces the rate of ATP hydrolysis (Klemm and Bell, 2001). Taking advantage of the fact that both residues are evolutionary conserved (NCBI, Conserved Domain Database), we produced the human homologues of the Walker A (K540T) and Walker B (D623Y) mutants. As indicated in Fig. 6A, mutation of K540 affected the

subnuclear distribution of Orc1p* suggesting the importance of ATP-binding. No effect was observed in the case of the D623Y mutant. The relevance of the Walker A domain was also verified in human HeLa cells by both immunofluorescence (not shown) and biochemical cell fractionation. As shown in Fig. 6D, although the wild-type Orc1p* was exclusively found in the chromatin (P3) fraction, half of the mutated protein was detectable in the soluble (S1) material indicating that the K540T substitution reduced the interaction of Orc1p* with chromatin
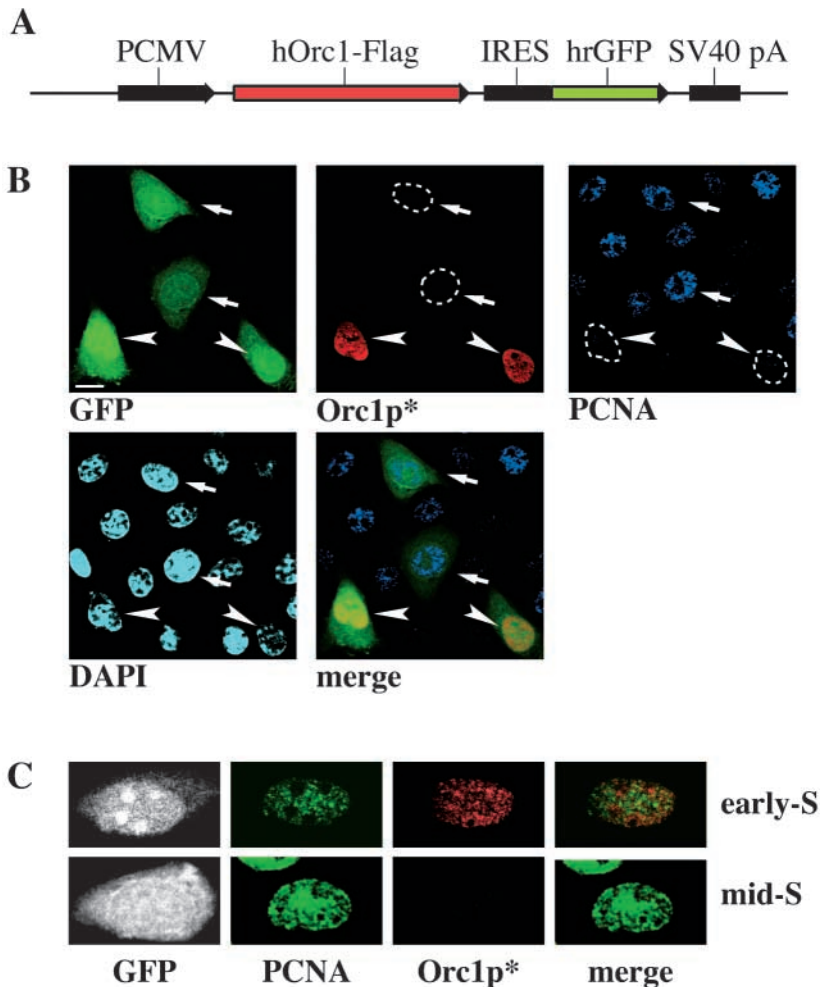

Fig. 4. Orc1p* in S-phase nuclei. HeLa cells were transfected with a plasmid that directs the expression of a dicistronic mRNA in which the sequence of Orc1-Flag is upstream of the GFP. (A) Schematic diagram of the pOrc1-Flag/GFP plasmid. PCMV, cytomegalovirus promoter; IRES, internal ribosomal entry site; SV40 pA, SV40-derived RNA processing site. (B) Cells were co-stained with the anti-Flag polyclonal and anti-PCNA monoclonal antibodies. Antibodies were revealed with the TRITC-conjugated anti-rabbit and Cy5-conjugated anti-mouse secondary antibodies. Nuclei were stained with DAPI. Confocal laser images were taken. The overlay of GFP (visualized in green), Orc1-Flag (red) and PCNA (blue) is shown (merge). The arrows indicate PCNA-positive GFP-positive nuclei in which Orc1-Flag is not detectable. Arrowheads show transfected nuclei expressing Orc1-Flag that are PCNA-negative. To preserve the GFP signal, we skipped Triton extraction before fixation. Under these conditions PCNA staining was detectable not only in S-phase replicative patterns but also in G2-phase cells characterized by intense homogenous staining. Bar, 10 μm. (C) Shows a PCNA-positive, Orc1p*-positive nucleus in early S phase (early-S) and a PCNA-positive, Orc1p*-negative nucleus in mid S phase (mid-S). The merged images show that in early S phase, Orc1p* does not colocalize with PCNA.
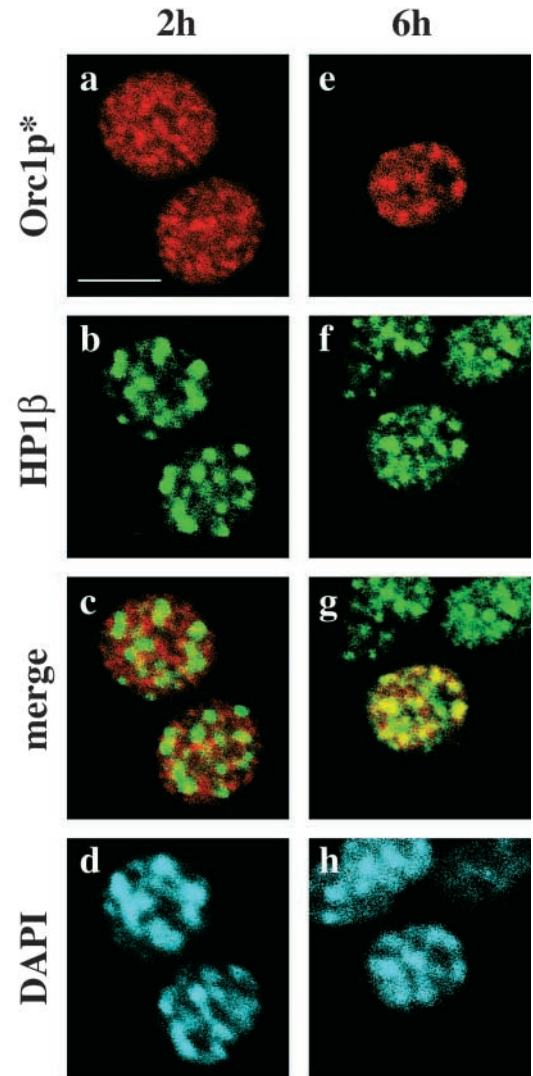

Fig. 5. Orc1p* in G1-phase nuclei. (a-h) Transiently transfected NIH-3T3 cells were blocked at the mitotic spindle checkpoint with nocodazole and allowed to recover for 2 hours (a-d) and 6 hours (e-h). Fixed cells were incubated with the rabbit anti-Flag polyclonal antibody (a,e), and with the anti-HP1β antibody (b,f). Antibodies were revealed with the anti-rabbit TRITC-conjugated (red) and with the anti-rat Cy5-conjugated (green) antibodies. Confocal laser images are shown. The overlay of Orc1p* (red) and HP1β (green) is also shown (merge). Chromatin was stained with DAPI (d,h). Bar, 10 μm.

to approximately 50%. No effect was detectable by co-immunoprecipitation in the nuclear cell extract on the ability of Orc1p* to interact with Orc2p (Fig. 6E).

During the characterization of these mutants we realized that, as indicated in Fig. 6A, removal of residues 151-269 affected the nuclear accumulation of the protein. The analysis of this sequence with the PSORT II program identified a putative nuclear localization signal (NLS) starting at residue 259 (PGRIKRKV). Replacement of amino acids RKV with three alanine residues (mutant $A^{264,265,266}$) was sufficient to hamper nuclear accumulation and the mutated protein was cytoplasmic (Fig. 6C) or distributed to the whole cell body (not shown) in more than 60% of the transfected cells. The failure to completely abrogate nuclear localization (Fig. 6C, right side)

however, suggests that additional motifs can mediate nuclear import of $A^{264,265,266}$. Although it showed an altered distribution, this mutant as well as Δ151-269, was still degraded in S phase similar to the wild-type protein (not shown). This indicates that degradation of Orc1p during the cell cycle does not require nuclear accumulation.

In vitro interaction between human Orc1p and HP1

The results in the previous section identified two regions involved in the association of Orc1p with heterochromatin, one of which is located at the N-terminus of the protein. In both *S. cerevisiae* and in *Drosophila* the N-terminal region of Orc1p is involved in the interaction with Sir1/ HP1 proteins (Pak et

Fig. 6. Analysis of Orc1p mutants. (A) All mutants were fused to either GFP or Flag-epitope and their subcellular distribution was assessed in transiently transfected NIH-3T3 cells. The region of human Orc1p included in each fusion is indicated by the corresponding amino acids on the left hand side. Internal deletion mutants are indicated with a Δ symbol. Substitution mutants are indicated by the corresponding single-code amino acid letter. Black bars indicate substituted residues. The ability of each mutant to accumulate at DAPI foci was scored as + (targeting proficient) or – (targeting deficient). The localization in cell nucleus (N) or in the cytoplasm (C) is indicated. A diagram including the main functional domains of the protein is shown at the top. BAH, bromo-adjacent-homology domain; HP1, HP1-binding site (Pak et al., 1997); Sir1, Sir1-binding site (Zhang et al., 2002a); AAA, ATPase domain; HW, putative DNA binding site (Liu et al., 2000). (B) Immunolocalization of the Δ151-269 mutant fused to the Flag epitope in NIH-3T3 cells. Chromatin was stained with DAPI. Confocal laser images of the same field were taken and merged. (C) Immunolocalization of the $A^{264,265,266}$ mutant fused to the Flag epitope in NIH-3T3 cells. Images show cells with cytoplasmic (left) or nuclear (right) distribution of the overexpressed protein. Chromatin was stained with DAPI. Confocal laser images were taken. Bar, 10 μm. (D) Chromatin-binding of Orc1p* (wt) and Orc1-K540T-Flag (K540T) mutant was analyzed by western blotting with the anti-Flag antibody. Transiently transfected HeLa cells were synchronized in G1-phase and fractionated as described in Materials and Methods. The amount of protein in the chromatin (P3) and soluble fractions (S1) was compared for each construct. The amount of P3 fraction analyzed for each sample was corrected for the efficiency of transfection determined by measuring in parallel the fraction of Orc1p* expressing cells. The level of endogenous Orc2p in the loaded P3 fractions is also shown. TE, total cell extracts. (E) Nuclear extracts (NE) of HeLa cells expressing K540T-Flag epitope (+) and of non-transfected cells (–) were probed with the anti-Flag polyclonal antibody and the anti-Orc2 polyclonal antibody. The same extracts were used in co-immunoprecipitation experiments with the monoclonal anti-Flag M2 affinity gel (IP). The presence of Orc1-Flag and of Orc2p in the immunoprecipitate was revealed by western blotting with anti-Flag and anti-Orc2 polyclonal antibodies.
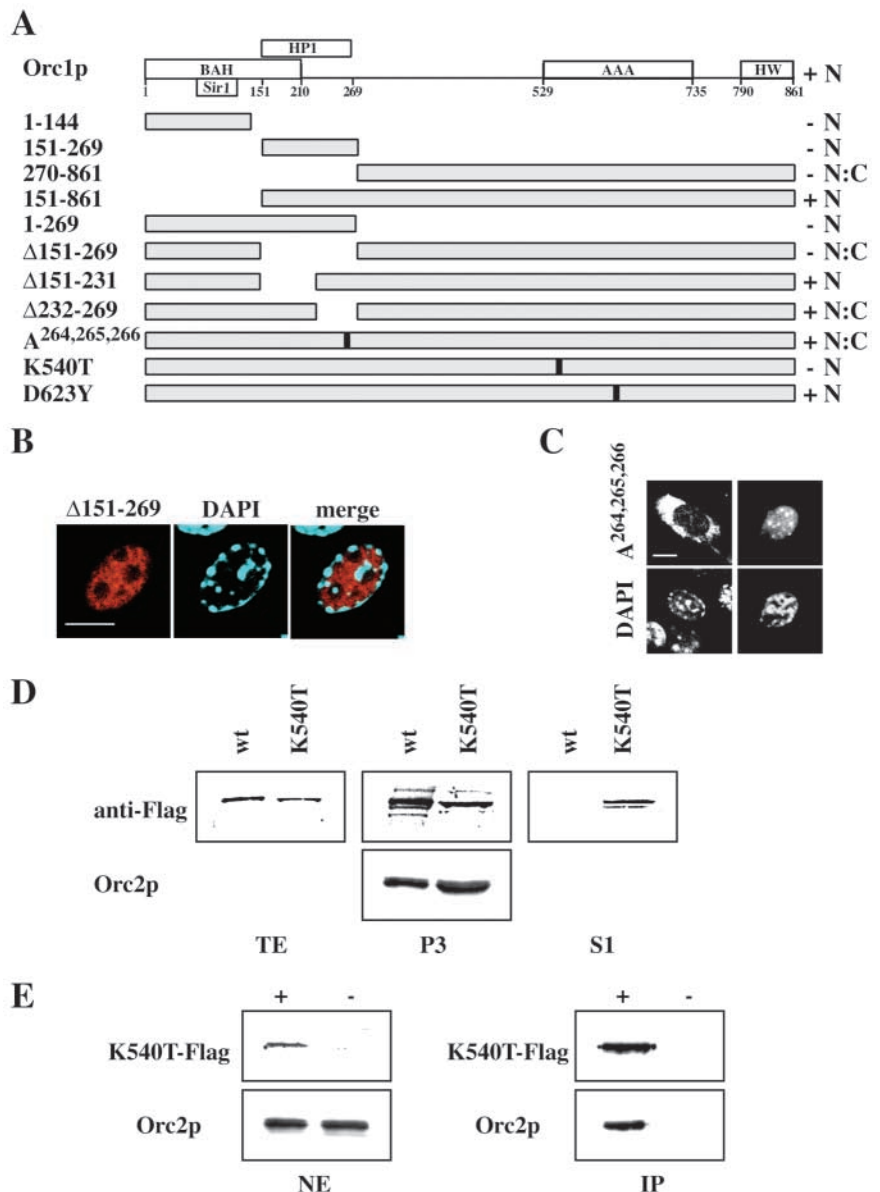
al., 1997; Zhang et al., 2002a). We thus asked whether the 151-269 region of human Orc1p could play the same role. In vitro translated [^{35}S]-labeled human Orc1p and Orc2p were challenged for their ability to bind a GST-HP1α fusion. As shown in Fig. 7A, Orc1p (upper panel, left side) but not Orc2p (upper panel, right side) was specifically retained on agarose beads loaded with GST-HP1α but not on beads loaded with GST alone (see quantification of the radioactive signals in Fig.

7B). Next, we performed a similar GST pull-down experiment by using a series of in vitro translated proteins corresponding to different portions of human Orc1p. As shown in Fig. 7C and quantified in Fig. 7D, binding to HP1α required amino acids 151-269 of Orc1p. This conclusion is consistent with the in vitro analysis of the interaction between *Drosophila* Orc1p and HP1 proteins (Pak et al., 1997) and raises the possibility that HP1 might have a role in Orc1p focalization.

Fig. 7. Orc1p but not Orc2p binds to HP1. (A) GST pull-down experiment performed by incubating 2 µg of either GST or GST-HP1α immobilized on glutathione-agarose beads with in vitro translated [^{35}S]-labeled Orc1p or Orc2p. After binding at 4°C, the beads were extensively washed and bound proteins were loaded onto a 10% acrylamide-SDS gel. The upper panel shows the autoradiograph; the lower panel shows the gel after staining with Coomassie blue. The input lanes contain the labeled proteins prior to binding. (B) Quantification of the GST pull-down experiment from A. The amount of radioactivity bound to the beads is indicated as a percentage of the input material. (C) HP1α binds to a region of Orc1p encompassing amino acids 151-269. The indicated [^{35}S]-labeled deletion mutants of Orc1p were incubated with either GST or GST-HP1α and processed as described in A. (D) Quantification of the GST pull-down experiment of panel C. (E) Visualization of FRET in human HeLa cells. The plasmids indicated on top of each column were transfected in asynchronous HeLa cells; individual transfected cells were visualized by excitation at 480 nm and collection at 520 nm, showing EGFP fluorescence after direct EGFP excitation (panels in row a), and by excitation at 350 nm and collection at 520 nm, showing EGFP fluorescence after BFP excitation, indicating FRET (panels in row b). (F) Quantification of FRET between EGFP-HP1α and BFP-Orc1. Fluorescent emission at 520 nm from individual cells transfected with the indicated constructs was recorded after excitation at 350 or 480 nm, and integrated intensities over the whole cell were evaluated. The plotted values (indicated by dots) represent the ratio between these two measurements: higher values indicate more efficient resonant energy transfer between BFP and EGFP. Ten consecutively analyzed cells were considered for each transfection; both their individual fluorescence ratios and their percentile box plot distributions are shown. In each box, the horizontal lines from top to bottom mark the 10th, 25th, 75th and 90th percentiles. Cells transfected with pEGFP-HP1α and pBFP-Orc1 plasmids showed FRET between the two fluorescent proteins that was dependent on the presence of both the HP1α and Orc1p moieties, thus indicating binding between these two proteins in vivo.
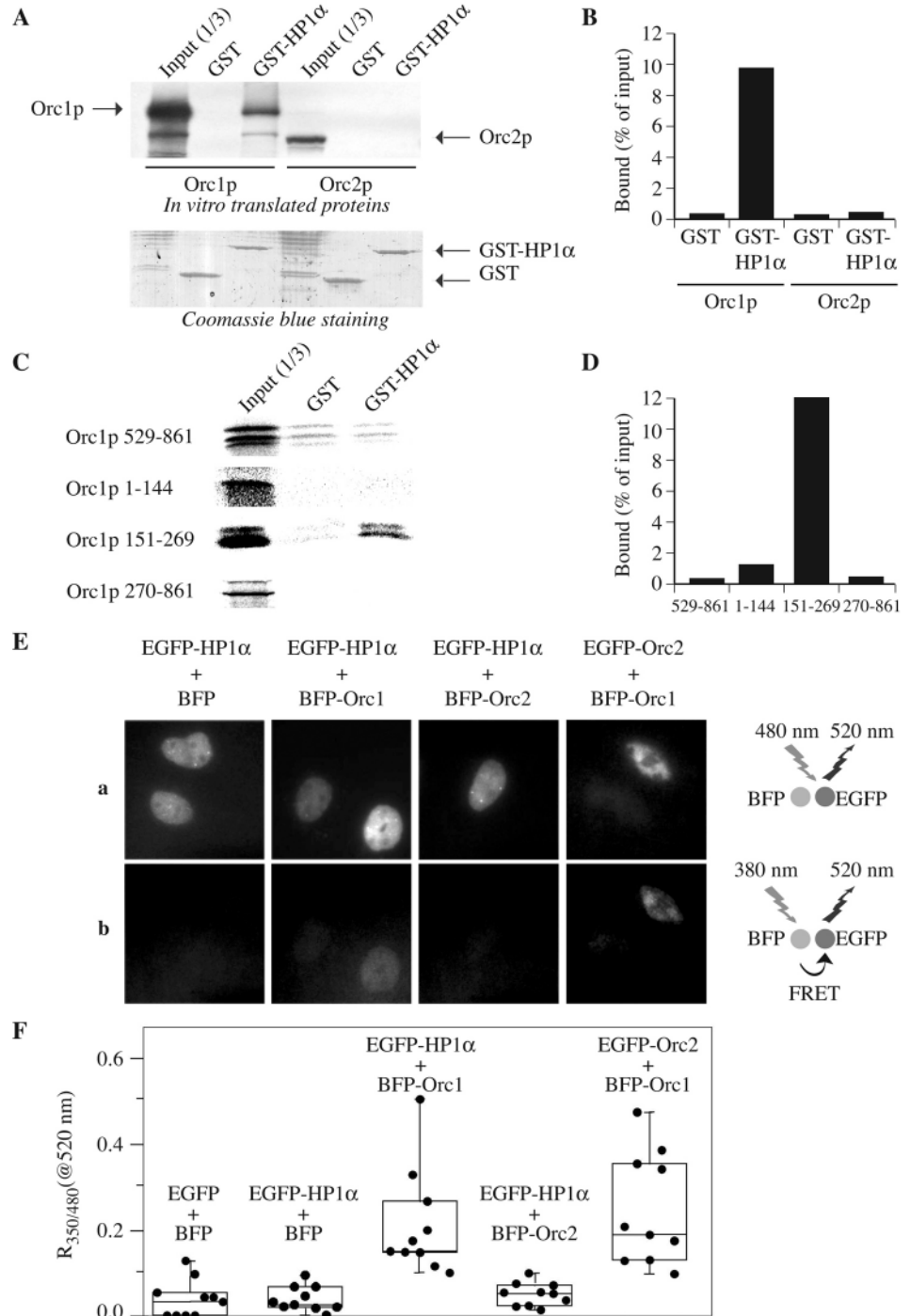
Visualization of direct Orc1p-HP1 interaction in human cells by FRET

A powerful technique to study the formation of specific protein complexes inside the cells is based on fluorescence resonant energy transfer (FRET) between two interacting proteins tagged with optically matched pairs of fluorophores; the presence of FRET indicates protein-protein interaction at distances in the order of a nanometer (Day, 1998; Selvin, 2000; van Roessel and Brand, 2002). We decided to apply this methodology to investigate the in vivo interaction between Orc1p and HP1. FRET experiments were performed by transfection of human HeLa cells with plasmids expressing HP1α and Orc1p fused at their N-terminus with EGFP and BFP respectively. We have already observed that the BFP:EGFP fluorescent protein pair has excitation and emission properties favorable for FRET and we have exploited these properties to study the in vivo interactions of other nuclear proteins in the same experimental conditions (Marcello et al., 2001; Marcello et al., 2003). FRET image analysis of individual transfected cells are shown in Fig. 7E. Upper panels show the intracellular distribution of fluorescence at 520 nm (the peak wavelength of EGFP emission) under excitation at 480 nm; lower panels show the fluorescence of the same fields after excitation of BFP at 350 nm. Under these conditions, only cells expressing EGFP-HP1α together with BFP-Orc1, but not with BFP alone or BFP fused to Orc2, could be visualized. Detailed quantitative analysis of several cells transfected with the different protein pairs are presented in Fig. 7F, which shows the experimental FRET signal and its distribution. All the cells transfected with EGFP-HP1α and BFP-Orc1 showed FRET values higher than those detected in the control transfections ($P<0.001$), indicating direct interaction between the two proteins. In the same set of experiments, FRET was also found positive between EGFP-Orc1 and BFP-Orc2, further supporting the direct binding of the two proteins in vivo.

Orc1p focalization survives TSA and RNase A treatments

The results in the previous sections indicate that the association of Orc1p with heterochromatin requires a protein region that mediates the interaction with HP1. We asked whether HP1 was necessary for the stable association of Orc1p with heterochromatin. It has recently been described that treatment of mouse cells with trichostatin A (TSA), an inhibitor of histone-deacetylase, induces redistribution of HP1 owing to a loss of HP1-binding sites in acetylated pericentric regions (Maison et al., 2002). We analyzed the localization of Orc1-Flag and of the endogenous HP1α in transiently transfected NIH-3T3 cells after TSA treatment. As shown in Fig. 8, TSA treatment (6 hours of growth in 0.5 µg/ml) triggered the redistribution of HP1 (Fig. 8A) without affecting the association of Orc1p* with DAPI bright spots (Fig. 8B). This was also confirmed by biochemical cell fractionation (see Fig. S5 in supplementary material).

An RNA component has recently been described as a crucial parameter involved in the maintenance of higher-order chromatin structure at pericentric heterochromatin (Maison et al., 2002; Muchardt et al., 2002). Cell treatment with RNase A induced the displacement of HP1 from heterochromatic regions whereas DAPI staining corresponding to pericentric
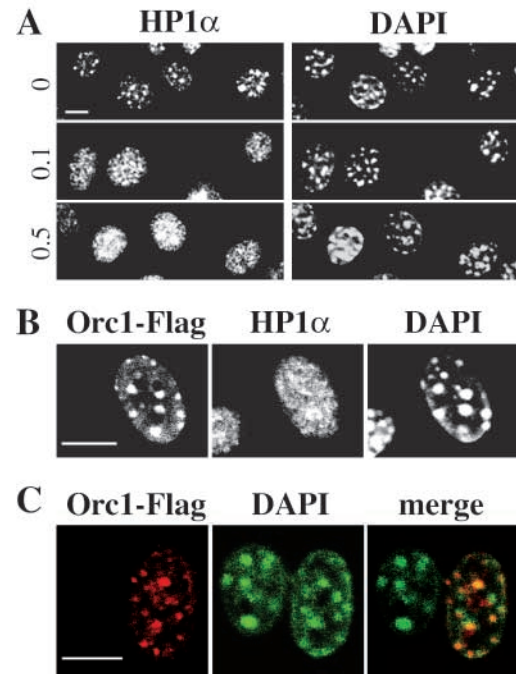

Fig. 8. Orc1p* focalization survives TSA and RNase treatment. (A) NIH-3T3 cells were treated with 0, 0.1 and 0.5 µg/ml TSA for 6 hours. Fixed cells were stained with the anti-HP1α antibody. Heterochromatin was stained with DAPI. Dispersal of HP1 from DAPI foci is already detectable at 0.1 µg/ml TSA. (B) Cells expressing Orc1-Flag were incubated in the presence of 0.5 µg/ml TSA as in panel A. Fixed cells were co-stained with the anti-Flag and anti-HP1α antibodies. Heterochromatin was stained with DAPI. In contrast to HP1, Orc1-Flag still colocalizes with DAPI foci. (C) Cells expressing Orc1-Flag were incubated with RNase A as described in Materials and Methods. Orc1-Flag was visualized with the anti-Flag antibody; heterochromatin was stained with DAPI visualized in green for a better resolution of the merged image. Confocal laser images are shown. Bar, 10 µm.

regions was essentially preserved (not shown). The same treatment, however, had no effect on the distribution of Orc1-Flag and the protein was still accumulated at pericentric heterochromatin (Fig. 8C). Thus, the association of Orc1p with DAPI bright spots survives treatments that displace HP1. Collectively these results suggest a model whereby HP1 is involved in the recruitment of Orc1p* to heterochromatin. Thereafter, binding of Orc1p* to AT-rich sequences in DAPI-stained DNA would make the association with heterochromatin HP1-independent.

Discussion

Orc1p seems to have a regulatory role in the assembly of the ORC in human cells. However, the characterization of its function is still limited. This is partially due to the lack of suitable antibodies, which has so far hampered the analysis of the subnuclear distribution. Moreover, a few contradictory reports have been published in the last few years about the protein stability in mammals. According to some authors, the protein is permanently bound to the origins and its level remains constant throughout the cell cycle (Okuno et al., 2001).

On the other hand, others suggest that Orc1p is displaced from chromatin after origin firing, but it is still controversial whether the displaced protein is eventually degraded by the proteasome (Araki et al., 2003; Kreitz et al., 2001; Mendez et al., 2002; Sun et al., 2002; Tatsumi et al., 2003). Here we have investigated the behavior of epitope-tagged human Orc1p overexpressed in mammalian cells (Orc1p*). Orc1p* shows important features of the endogenous protein: it interacts with Orc2p, another subunit of ORC, and binds to a well-characterized origin of DNA replication.

By applying an approach that does not entail cell synchronization (Fig. 4; see also Fig. S2 in supplementary material) we have shown that the level of Orc1p* is regulated during the cell cycle. This is in line with that previously reported for the endogenous protein (Mendez et al., 2002) and rules out the possibility that Orc1p degradation takes place during the preparation of cell extracts. Moreover, our analysis indicates that the level of Orc1p* is regulated both in human and mouse cells. This raises the possibility that the different regulation of Orc1p observed in different mammalian species could be caused by the divergence of the protein sequence (65.8% identity between the human and mouse protein, EMBL-EBI ClustalW program). Finally, our results suggest that degradation of Orc1p during S phase follows a precise program. The level of Orc1p* decreases during the S phase and the protein is no longer detectable in mid- and late-S-phase nuclei (Fig. 4). Moreover, in early S phase, Orc1p* does not colocalize with replication factories stained by PCNA. This is in agreement with a model whereby origin firing is accompanied by the displacement and degradation of Orc1p to prevent re-replication during S phase.

Orc1p and heterochromatin

Another interesting observation concerns the association of Orc1p* with heterochromatin in mid and late G1. The association of ORC with transcriptionally silenced, late replicating portions of the genome has been observed in other organisms, where ORC seems to play an active role in the assembly of these chromatin conformations. In the yeast *S. cerevisiae*, ORC binding to an ARS element is required for the recruitment of Sir factors and hence for the transcriptional silencing of the HML locus (Vujcic et al., 1999). In *Drosophila,* mutations of Orc2p were shown to perturb HP1 localization (Huang et al., 1998; Pak et al., 1997). Finally, it has been reported that human Orc2p binds in vivo to α-satellite sequences that compose pericentric heterochromatin (Keller et al., 2002). We have added a few molecular details to the characterization of the association of Orc1p with heterochromatin and we have identified two protein domains that are involved in this phenomenon. The first one (amino acids 151-269) mediates the in vitro interaction with HP1, a component of heterochromatin. This finding extends to the human protein the ability to interact with heterochromatic proteins previously demonstrated in budding yeast and *Drosophila* (Pak et al., 1997; Zhang et al., 2002a). In these systems, ORC acts as the recruiter whereas the opposite apparently occurs in humans. Indeed, the association of Orc1p* with heterochromatin is temporally delayed with respect to HP1 (Fig. 5) and requires the HP1 binding domain. Surprisingly, the displacement of HP1 from heterochromatin

induced by deacetylase inhibitors or by RNase A (Maison et al., 2002; Muchardt et al., 2002) does not affect Orc1p localization (Fig. 8). We hypothesize that HP1 plays a role in the recruitment, but not in the stable association of Orc1p with heterochromatin, which might be mediated by interactions with other components of these nuclear districts, one possible candidate being the AT-rich repeated DNA elements. This is also suggested by the identification of the Walker A motif as the second domain involved in the subnuclear localization of Orc1p. Indeed, a mutation in this motif that abrogates ATP binding reduces both the affinity of ORC for DNA (Chesnokov et al., 2001) and the association of Orc1p with heterochromatin.

The amount of endogenous Orc1p is tightly controlled and the number of Orc1p molecules approximately corresponds to the estimated number of replication origins (Kreitz et al., 2001). Thus, Orc1p* focalization could reflect the behavior of excess protein that does not participate to replication competent ORCs. However, the nature of the two domains involved in the association with heterochromatin suggests that this distribution could be functionally relevant. Human ORC displays limited, if any, sequence specificity of binding to DNA. This implies that the selection of specific DNA replication origins must rely on other factors such as chromatin proteins or transcription factors that might help the association of ORC with DNA (Vashee et al., 2003). In this perspective, HP1 could have a role in targeting ORC to heterochromatin thus improving the replication of highly compacted DNA regions. On the other hand, heterochromatin could represent a sort of buffer to sequester the surplus of Orc1p* until degradation in S phase. This could be part of a mechanism that finely tunes the selection of DNA replication origins operating during the cell cycle, and which becomes more evident under our experimental conditions.

The meaning of the association of Orc1p with heterochromatin is still obscure. Heterochromatin has evolved as a nuclear domain to silence expressed genes by sequestering them in compartments not accessible to transcription factors. It is possible that ORC could play a major role in coordinating DNA replication with the chromatin organization and the expression pattern of the genome. This possibility is consistent with the capacity of Orc1p to interact with proteins such as Noc3 and histone acetyl-transferase HBO1, enabling the modulation of chromatin structure (Iizuka and Stillman, 1999; Zhang et al., 2002b). Growing experimental evidence indicates that initiation of DNA replication in higher eukaryotes does not simply depend on sequence elements but also depends on important parameters such as the packaging status and the nuclear position of chromatin. ORC is a good candidate to link all these different aspects acting as a chromatin remodeling factor.

References

Abdurashidova, G., Danailov, M., Ochem, G., Triolo, G., Djeliova, S., Radulescu, A., Vindigni, A., Riva, S. and Falaschi, A. (2003). Localization of proteins bound to a replication origin of human DNA along the cell cycle. *EMBO J.* **22**, 4294-4303.

Araki, M., Wharton, R., Tang, Z., Yu, H. and Asano, M. (2003). Degradation of origin recognition complex large subunit by the anaphase-promoting complex in *Drosophila. EMBO J.* **22**, 6115-6126.

Bell, S. and Dutta, A. (2002). DNA replication in eukaryotic cells. *Annu. Rev. Biochem.* **71**, 333-374.

Bell, S. and Stillman, B. (1992). ATP-dependent recognition of eukaryotic origin of DNA replication by a multiprotein complex. *Nature* **357**, 128-134.

Biamonti, G., Paixão, S., Montecucco, A., Peverali, F., Riva, S. and Falaschi, A. (2003). Is DNA sequence sufficient to specify DNA replication origins in metazoan cells? *Chromosome Res.* **11**, 403-412.

Chesnokov, I., Remus, D. and Botchan, M. (2001). Functional analysis of mutants and wild-type Drosophila origin recognition complex. *Proc. Natl. Acad. Sci. USA* **98**, 11997-12002.

Chiodi, I., Biggiogera, M., Denegri, M., Corioni, M., Weighardt, F., Cobianchi, F., Riva, S. and Biamonti, G. (2000). Stress-induced nuclear bodies are sites of accumulation of pre-mRNA processing. *J. Cell Sci.* **113**, 4043-4053.

Day, R. (1998). Visualization of Pit-1 transcription factor interactions in the living cell nucleus by fluorescence resonance energy transfer microscopy. *Mol. Endocrinol.* **12**, 1410-1419.

Frouin, I., Montecucco, A., Biamonti, G., Hubscher, U., Spadari, S. and Maga, G. (2002). Cell cycle-dependent dynamic association of cyclin/Cdk complexes with human DNA replication proteins. *EMBO J.* **21**, 2485-2495.

Giacca, M., Zentilin, L., Norio, P., Diviacco, S., Dimitrova, D., Contreas, G., Biamonti, G., Perini, G., Weighardt, F., Riva, S. et al. (1994). Fine mapping of a replication origin of human DNA. *Proc. Natl. Acad. Sci. USA* **91**, 7119-7123.

Huang, D. W., Fanti, L., Pak, D. T. S., Botchan, M. R., Pimpinelli, S. and Kellum, R. (1998). Distinct cytoplasmic and nuclear fractions of Drosophila heterochromatin protein 1, their phosphorylation levels and associations with origin recognition complex proteins. *J. Cell Biol.* **142**, 307-318.

Iizuka, M. and Stillman, B. (1999). Histone acetyltransferase HBO1 interacts with ORC1 subunit of the human initiator protein. *J. Biol. Chem.* **274**, 23027-23034.

Jones, D. O., Cowell, I. G. and Singh, P. B. (2000). Mammalian chromodomain proteins, their role in genome organisation and expression. *Bioessays* **22**, 124-137.

Keller, C., Ladenburger, E., Kremer, M. and Knippers, R. (2002). The origin recognition complex marks a replication origin in the human TOP1 gene promoter. *J. Biol. Chem.* **277**, 31430-31440.

Klemm, R. and Bell, S. (2001). ATP bound to the origin recognition complex is important for preRC formation. *Proc. Natl. Acad. Sci. USA* **98**, 8361-8367.

Kreitz, S., Ritzi, M., Baack, M. and Knippers, R. (2001). The human origin recognition complex protein 1 dissociates from chromatin during S phase in HeLa cells. *J. Biol. Chem.* **276**, 6337-6342.

Ladenburger, E.-M., Keller, C. and Knippers, R. (2002). Identification of a binding region for human origin recognition complex proteins 1 and 2 that coincides with an origin of DNA replication. *Mol. Cell. Biol.* **22**, 1036-1048.

Li, C.-J. and DePamphilis, M. (2002). Mammalian Orc1 protein is selectively released from chromatin and ubiquitinated during S-to-M transition in the cell division cycle. *Mol. Cell. Biol.* **22**, 105-116.

Liu, J., Smith, C., DeRyckere, D., DeAngelis, K., Martin, G. and Berger, J. (2000). Structure and function of cdc6/cdc18, implication for origin recognition and checkpoint control. *Mol. Cell* **6**, 637-648.

Maison, C., Bailly, D., Peters, A. H. F. M., Quivy, J.-P., Roche, D., Taddei, A., Lachner, M., Jenuwein, T. and Almouzni, G. (2002). Higher-order structure in pericentric heterochromatin involves a distinct pattern of histone modification and an RNA component. *Nat. Genet.* **30**, 329-334.

Marcello, A., Cinelli, R., Ferrari, A., Signorelli, A., Tyagi, M., Pellegrini, V., Beltram, F. and Giacca, M. (2001). Visualization of in vivo direct interaction between HIV-1 Tat and human cyclin T1 in specific subcellular compartments by fluorescence resonance energy transfer. *J. Biol. Chem.* **276**, 39220-39225.

Marcello, A., Ferrari, A., Pellegrini, V., Pegoraro, G., Lusic, M., Beltram, F. and Giacca, M. (2003). Recruitment of human cyclin T1 to nuclear bodies through direct in vivo interaction with the PML protein. *EMBO J.* **22**, 2156-2166.

Marzio, G., Tyagi, M., Gutierrez, M. and Giacca, M. (1998). HIV-1 Tat transactivator recruits p300 and CREB-binding protein histone acetyltransferases to the viral promoter. *Proc. Natl. Acad. Sci. USA* **95**, 13519-13524.

Mendez, J. and Stillman, B. (2000). Chromatin association of human origin recognition complex, cdc6, and minichromosome maintenance proteins during the cell cycle: assembly of prereplication complexes in late mitosis. *Mol. Cell. Biol.* **20**, 8602-8612.

Mendez, J., Zou-Yang, X., Kim, S.-Y., Hidaka, M., Tansey, W. and Stillman, B. (2002). Human origin recognition complex large subunit is degraded by ubiquitin-mediated proteolysis after initiation of DNA replication. *Mol. Cell* **9**, 481-491.

Montecucco, A., Rossi, R., Levin, D. S., Gary, R., Park, M. S., Motycka, T. A., Ciarrocchi, G., Villa, A., Biamonti, G. and Tomkinson, A. E. (1998). DNA ligase I is recruited to sites of DNA replication by an interaction with proliferating cell nuclear antigen, identification of a common targeting mechanism for the assembly of replication factories. *EMBO J.* **17**, 3786-3795.

Montecucco, A., Rossi, R., Ferrari, G., Scovassi, A. I., Prosperi, E. and Biamonti, G. (2001). Etoposide induces the dispersal of DNA ligase I from replication factories. *Mol. Biol. Cell* **12**, 2109-2118.

Muchardt, C., Guillemé, M., Seeler, J.-S., Trouche, D., Dejean, A. and Yaniv, M. (2002). Coordinated methyl and RNA binding is required for heterochromatin localization of mammalian HP1α. *EMBO Rep.* **3**, 975-981.

Okuno, Y., McNairn, A. J., den Elzen, N., Pines, J. and Gilbert, D. M. (2001). Stability, chromatin association and functional activity of mammalian pre-replication complex proteins during the cell cycle. *EMBO J.* **20**, 4263-4277.

Paixão, S., Colaluca, I., Cubells, M., Peverali, A., Destro, A., Giadrossi, S., Giacca, M., Falaschi, A., Riva, S. and Biamonti, G. (2004). Modular structure of the human lamin B2 replicator. *Mol. Cell. Biol.* **24**, 2958-2967.

Pak, D. S. T., Pflumm, M., Chesnokov, I., Huang, D. W., Kellum, R., Marr, J., Romanowski, P. and Botchan, M. R. (1997). Association of the origin recognition complex with heterochromatin and HP1 in higher eukaryotes. *Cell* **91**, 311-323.

Pasero, P., Bensimon, A. and Schwob, E. (2002). Single-molecule analysis reveals clustering and epigenetic regulation of replication origins at the yeast rDNA locus. *Genes Dev.* **16**, 2479-2484.

Rossi, R., Villa, A., Negri, C., Scovassi, I., Ciarrocchi, G., Biamonti, G. and Montecucco, A. (1999). The replication factory targeting sequence/PCNA-binding site is required in G(1) to control the phosphorylation status of DNA ligase I. *EMBO J.* **18**, 5745-5754.

Selvin, P. (2000). The renaissance of fluorescence resonance energy transfer. *Nat. Struct. Biol.* **7**, 730-734.

Sun, W.-H., Coleman, T. R. and DePamphilis, L. M. (2002). Cell cycle-dependent regulation of the association between origin recognition proteins and somatic cell chromatin. *EMBO J.* **21**, 1437-1446.

Tatsumi, Y., Ohta, S., Kimura, H., Tsurimoto, T. and Obuse, C. (2003). The ORC1 cycle in human cells. *J. Biol. Chem.* **278**, 41528-41534.

Thome, K., Dhar, S., Quintana, D., Delmolino, L., Shahsafaei, A. and Dutta, A. (2000). Subsets of human origin recognition complex (ORC) subunits are expressed in non-proliferating cells and associate with non-ORC proteins. *J. Biol. Chem.* **275**, 35233-35241.

van Roessel, P. and Brand, A. (2002). Imaging into the future, visualizing gene expression and protein interactions with fluorescent proteins. *Nat. Cell Biol.* **4**, E15-E20.

Vashee, S., Cvetic, C., Lu, W., Simancek, P., Kelly, T. and Walter, J. (2003). Sequence-independent DNA binding and replication initiation by the human origin recognition complex. *Genes Dev.* **17**, 1894-1908.

Vujcic, M., Miller, C. and Kowalski, D. (1999). Activation of silent replication origins at autonomously replicating sequence elements near the HML locus in budding yeast. *Mol. Cell. Biol.* **19**, 6098-6109.

Zhang, Z., Hayashi, M. K., Merkel, O., Stillman, B. and Xu, R.-M. (2002a). Structure and function of BAH-containing domain of Orc1p in epigenetic silencing. *EMBO J.* **21**, 4600-4611.

Zhang, Z., Yu, Z., Fu, X. and Liang, C. (2002b). Noc3p, a bHLH protein, plays an integral role in the initiation of DNA replication in budding yeast. *Cell* **109**, 849-860.